Laser Chem. 1988, Vol. 9, pp. 317–337

Laser Induced Fluorescence of 4-*N,N*-Dimethylaminobenzonitrile (DMABN) and Related Compounds

ANITA C. JONES and DAVID PHILLIPS

The Royal Institution, 21 Albemarle Street, London W1X 4BS

(Received 20 May, 1988)

The role of polar solvent in determining the photophysics of normal (b^*) and anomalous (a^*) fluorescence from 4-*N,N*-dimethylaminobenzonitrile (DMABN) and related compounds has been investigated by means of picosecond time-resolved fluorescence studies in non-polar/polar solvent mixtures, and by electronic spectroscopic studies on complexes of 1:1 stoichiometry prepared by nozzle expansion. The solution phase results indicate clearly that a DMABN-polar solvent complex is formed initially in either ground or excited state, and that this rearranges to a geometry from which the b^* to a^* state transition can occur. *Specific* solvent-solute interactions are clearly indicated by this work, and these lead to the necessity of modelling b^* state decay kinetics in solution by a *distribution* of decay times.

Laser induced fluorescence studies of jet-cooled solvated complexes of DMABN and the related molecule 4-aminobenzonitrile (4-ABN) provide evidence for the existence of 1:1 complexes involving interaction of a protic solvent molecule with either the cyano group or the amino group. In the case of 4-ABN both types of complex are fluorescent whereas in the case of DMABN, those complexes involving interaction with the dimethylamino group appear to be non-emissive. This behaviour may be due to formation of DMABN-solvent exciplex which constitutes a dark state under jet-cooled conditions. Neither the DMABN bare molecule nor the observed 1:1 solvated complexes exhibit a^* emission in the jet.

KEY WORDS: 4-N,N-dimethylaminobenzonitrile, 4-aminobenzonitrile, solute-solvent interactions, jet-cooled complexes, laser induced fluorescence.

INTRODUCTION

The fluorescence spectrum of *p*-dimethylaminobenzonitrile (DMABM) in polar solvents has two distinct bands, one the anomal-

ous (or a^*) emission, exhibits a very large Stokes shift, whereas the normal (or b^*) emission bears a mirror image relation to the absorption spectrum. The b^* emission is also observed in non-polar solvents, whereas the a^* emission is observed only in polar solvents. In low temperature glasses only the b^* emission is observed, irrespective of the medium. The origin of the a^* emission has been the subject of quite extensive theoretical and experimental investigations. Early work[1] ascribed this band to emission from the second excited singlet state, S_2, which was lowered in energy, below the S_1 state by solvent relaxation about its postulated large (~16 D) dipole moment. Subsequently Grabowski and co-workers[2] proposed that the a^* emission arose from a new state, a twisted intramolecular charge transfer (TICT) state, in which the dimethylamino group is twisted 90° with respect to the plane of the aromatic ring, and has transferred an electron to it (Figure 1). Such a state would have a large dipole moment, and would thus be stabilized in fluid polar solvents by means of the rapid (picosecond) solvent relaxation process. Thus the absence of the a^* emission in glasses and non-polar solvents, where isomerization and solvent stabilization do not occur, could be understood. Subsequent data[3,4] suggested that the TICT state had its origins in the ^1L_a state (S_2 in several derivatives related to DMABN), and thus the earlier work of Lippert and co-workers is compatible with the TICT model. This explanation was supported by many steady state experiments in pure polar solvents, particularly by the temperature dependence of the quantum yield of the a^* and b^* states.[5]

Picosecond time domain fluorescence studies lend support to the model outlined above.[5–10] It has been observed that the b^* state decays on a picosecond timescale with a rate that can be correlated with the

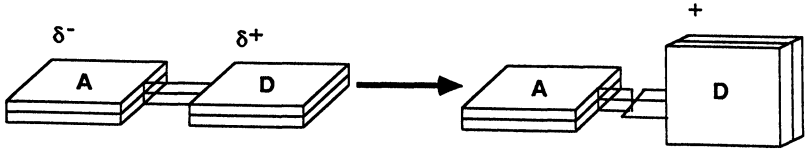

Figure 1 Schematic representation of the change in geometrical arrangement of donor group D and acceptor group A upon going from the B^* state to the TICT state. This transition involves (1) intramolecular rotation, (2) crossing of excited states and nonadiabatic coupling, (3) further charge transfer approaching a full electronic charge, and (4) relaxation of the polar solvent molecules around this increased dipole.

longitudinal relaxation time of the solvent[10] and the decay time of the b^* state is reflected in the rise time of the a^* emission.[6–8] More detailed studies have been made of the dynamics of the $b^* \rightarrow a^*$ reaction.[8–11]

Studies on three component systems (solute plus mixed polar/non-polar solvent) have led to alternative explanations however. In these three component systems the a^* emission can be observed at low concentrations of the polar solvent. Such low concentrations have a negligible effect on the bulk solvent dielectric constant, which is an important parameter in models invoking the solvent stabilization of a polar excited state, and thus an alternative model for DMABN fluorescence has been developed, the so-called exciplex model. This suggests that the a^* emission arises from a complex (or complexes) formed in an excited state reaction between DMABN and the polar solvent[12–14] and further proposes that three emissions are involved in the DMABN spectrum; a normal emission and that from two exciplexes, one planar, one twisted.

Although it is very clear that the polar solvent plays a crucial role in the photophysics of DMABN and related molecules, the exact nature of the interaction is as yet unclear. The present study, in two parts, was undertaken firstly to investigate further, using picosecond time-resolved fluorescence techniques, the ground and excited state interactions between DMABN and polar solvent in mixed bulk-phase solution, and secondly, to prepare in a supersonic nozzle expansion ground-state complexes of known, low stoichiometry of DMABN and related compounds and polar solvents in order to study in simplified circumstances the DMABN/solvent system. Preliminary results from both studies have been reported elsewhere,[15–18] and several reports of similar studies have recently appeared.[19–22]

EXPERIMENTAL

(a) Solution-phase studies

The time-resolved fluorescence of DMABN was measured using a time correlated single photon counting apparatus described in detail elsewhere.[23,24] The excitation source was a frequency doubled synchronously pumped cavity dumped rhodamine 6G dye laser. The instrument response function (mainly due to the photomultiplier) had

a width of about 600 picoseconds at the excitation wavelength, which was 293 nm. Energy resolved fluorescence decays were collected with rather high signal to noise ratio (typically 70–90,000 counts in the peak channel). They were analysed with the iterative least squares method[24] and quality of the fit was judged by criteria described in detail elsewhere.[24] Data were collected in 512 channels with a resolution of 16 and 36 psec/channel. Fluorescence was detected by an XP2020Q photomultiplier placed behind a ⅓ m monochromator. Data were collected with 4 nm (b^*) and 6 nm (a^*) resolution. It was ensured that the data were unchanged when a polarizer set at 54.7° to the excitation polarization was placed before the detection system.[15,16]

DMABN was purified by vacuum sublimation and recrystallization from cyclohexane. Solvents were purified by standard techniques and were non-fluorescent under the experimental conditions. The concentation of DMABN was typically 3×10^{-5} M. All samples were thoroughly degassed by several freeze-pump-thaw cycles, and were subsequently sealed off.

(b) Supersonic jet studies

4-ABN, DMABN and dimethylaniline (DMA) were obtained from Aldrich Ltd. and used without further purification. The supersonic jet apparatus has been described elsewhere.[25] Sample vapour, produced by heating the solid (4-ABN and DMABN) or liquid (DMA) sample in a temperature-controlled oven, was mixed with helium carrier gas, at a stagnation pressure of 3–4 Bar, and expanded through a continuous flow nozzle of diameter 100 μm. The complexing solvent was introduced into the expansion by passing a controlled fraction of the carrier gas flow through a high pressure reservoir containing the solvent. The solvents used were of analytical grade and were not purified further.

The excitation source was an excimer-pumped dye laser (Lambda Physik EMG 103MSC/FL2002) with bandwidth ≤ 0.2 cm^{-1}. For the measurement of excitation spectra, total fluorescence was collected with an $f/1$ lens and focussed onto a photomultiplier tube (EM1 XP2020Q). The photomultiplier output was processed by a Stanford Research Systems boxcar averager interfaced to an ARC microcomputer. Spectra were corrected for variation in laser intensity. Fluorescence spectra were recorded by wavelength dispersing the fluorescence through a 1 m monochromator (Hilger Monospek 1000).

Fluorescence was then detected by a Hamamatsu R928 photomultiplier and processed as above.

Fluorescence lifetimes in the jet were measured using the time-correlated single-photon counting technique as above, except that fluorescence was detected by a Hamamatsu R1564U microchannel plate photomultiplier (response function 140 ps fwhm). χ_v^2 values were typically ≤ 1.2, although higher values were accepted for low intensity signals such as the DMABN-CH_3OH complex fluorescence.

Quantum chemical calculations on the Hartree-Fock level were performed using the semi-empirical AM1 (Austin Model 1) method.[26] AM1 was derived from the MNDO (Modified Neglect of Diatomic Differential Overlap) method by modifying the core repulsion function to overcome the tendency of MNDO to overestimate the repulsions between atoms when at *ca.* their Van der Waals distances apart. The major advantage of AM1 over MNDO of interest here is the ability of AM1 to reproduce hydrogen bonds. The AM1 method was used to obtain optimized geometries of the bare molecules and 4-ABN-water complexes. In the computer program used, the geometries are defined in terms of bond lengths, bond angles and dihedral angles and optimization is achieved by the Davidson Fletcher Powell variable metric method; molecular symmetry can be imposed and specified variables held constant during the optimization.

RESULTS AND DISCUSSION

(a) Solution-phase results

Attempts were made to fit the fluorescence decays of DMABN in cyclohexane plus 0.5 M ethanol, butanol and acetonitrile to single component and dual component decays but the resulting fits were unacceptable.[15,16] A three-component fit could reproduce the data empirically, as shown in Table I.[15] However, it is well-known that such empirical fits can mimic many diverse forms of decay kinetics,[27,28] and stringent testing of models is called for here. The simplest scheme for DMABN fluorescence is shown in Scheme 1, but this has been shown *not* to be compatible with the observed data even if the transient diffusional term is k_3 is taken into account. The full discussion of these results will not be reproduced here, but the data have similarly been

Table I Decay parameters of DMABN/ethanol system. 0.04 ns/channel. (A) Fit to a bi-exponential function. (B) Fit to a three-exponential function.

	[EtOH] (M)	λ (nm)	Δt[a] (ns)	A_1	τ_1(ns)	A_2	τ_2(ns)	χ_v^{2}[b]
(A)	0.4	340	0.08	1.5	1.1	0.6	2.6	1.5
		340	0.8	1.5	1.3	0.4	2.9	1.1
		340	2.4	1.5	1.4	0.3	3.3	1.0
		520	0.0	−1.9	1.5	0.3	3.5	1.2
		520[c]	4.4		3.5			1.1
	0.8	340	0.04	2.2	0.7	0.4	2.5	2.8
		340	1.2	1.6	0.9	0.2	2.9	1.0
		520	0.0	−1.6	1.1	0.3	3.3	1.4
		520[c]	4.0		3.3			
(B)		A_1	τ_1(ns)	A_2	τ_2(ns)	A_3	τ_3(ns)	χ_v^2
	0.4	0.7[d]	0.6[d]	1.3	1.6	0.2	3.4	1.0
	0.8	1.5[d]	0.3[d]	1.4	0.9	0.2	2.9	1.0

[a] Time after the peak of the excitation pulse that the fit was started.
[b] Reduced chi-square.
[c] Fit to a single-exponential function.
[d] ±30%.

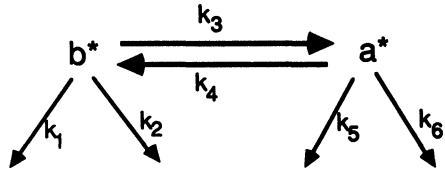

Scheme 1

shown to be not wholly compatible with the more complex "exciplex" model of Visser *et al.*[13,14] Scheme 2. Instead, results lead to the conclusion that the fluorescence decay of the *b** state in DMABN is best characterized by a distribution of decay times. This conclusion arose not only because the decay functions arising from the alternative models do not fit the data, but also because any data that could be extracted from these analyses were neither qualitatively nor quantitatively interpretable within the terms of a physically reasonable kinetic model. Similarly it was not possible to analyse meaningfully the data

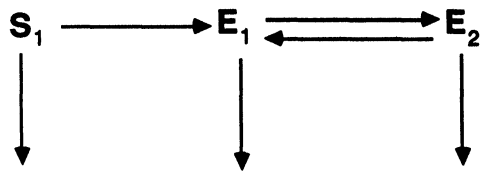

where S_1 represents the bare DMABN, E_1 is a planar exciplex and E_2 a twisted one.

Scheme 2

obtained from the three exponential analyses, although good quality fits were observed, as in Table I.

One approach to the analysis of a distribution of decay rates is to employ a fractional power exponential.

$$I_b^*(t) = A \exp\left[-(t/\tau)^{\beta}\right] \tag{1}$$

where $0 < \beta < 1$ and τ is a characteristic decay time. The value of β is directly related to the width of the distribution; a decreasing β implies a more significant departure from exponential decay, and thus a broader distribution of decay times. Equation (1), variously called the Kohlrausch[29] or William-Watts[30,31] function, has been applied to the analysis of the complex kinetics observed in, for example, photon correlation spectroscopy and hydrogen abstraction reactions. With (1) an average relaxation time, $\langle\tau\rangle$, may be defined:

$$\langle\tau\rangle = \frac{\tau}{\beta}\Gamma\left(\frac{1}{\beta}\right) \tag{2}$$

with $\Gamma(x)$ being the gamma function.

To analyse the experimental data, undistorted, noise free, decay profiles were first obtained. This was done by deconvolution with a multi-exponential function in this case, a sum of three exponentials, with all six parameters freely varying. β was then obtained from the slope of $\ln \ln [I(o)/I(t)]$ against $\ln t$, where $I(t)$ is the deconvoluted data set and $I(o)$ is obtained by extrapolation of the early time data. This analysis was only attempted for the butanol co-solvent samples, and the results are shown in Table II and Figure 2.

For concentration of butanol ≤ 0.5 M the quality of the fit was quite good (as judged by visual inspection, Figure 2). For the 0.9 M sample

Table II Concentration dependence of the (deconvuluted) b^* decay of DMABN plus butanol co-solvent, fit to Eq. (1).

[BuOH]/M	$\langle\tau\rangle$/ns	β
0.2	2.43	0.90
0.25	1.89	0.79
0.5	1.28	0.65
0.9	0.81	0.56

where were significant deviations at very early times. This could be caused either by the increased uncertainty in obtaining $I(o)$ when $I(t)$ is changing very rapidly with time, or by inadequacies in the data analysis procedure; possibly a sum of three exponential terms is insufficient to describe a true distribution of decay rates.

The trend in Table II is clear. The departure from the single exponential behaviour ($\beta = 1$), becomes more marked (decreasing β) with increasing concentrations of butanol. We note that when <0.1 M [BuOH] is used very little quenching of the b^* emission was observed, and the decay was very close to exponential. Thus the observed decay kinetics change from a homogeneous decay in pure cyclohexane to increasingly heterogenous kinetics in mixed solvents. As would be expected the mean lifetime $\langle\tau\rangle$ decreases with increasing concentration of alcohol. The very complex nature of the b^* emission kinetics would be expected to result in the observed disagreement between the b^* decay and the a^* risetime, when these are analysed in terms of a simple sum or difference of exponentials.

Heterogeneous decays can have two distinct origins. Firstly, the apparently time dependent form of a decay described by Eq. (1) may arise from a distribution of decay processes, which are in themselves time independent. Alternatively, a truly dynamic process, involving a sequence of correlated steps along a reaction co-ordinate may also result in a decay profile which will be well fit by Eq. (1). In principle the second alternative could be an appropriate description of an isomerization reaction, such as TICT state formation. However, because these measurements were made in fluid solvents, where the isomerization and related solvent motion will be fast (picoseconds), it is more likely that the observed complex kinetics, which persist on at least a nanosecond timescale, result from the first alternative, a distribution of first order reaction rates.

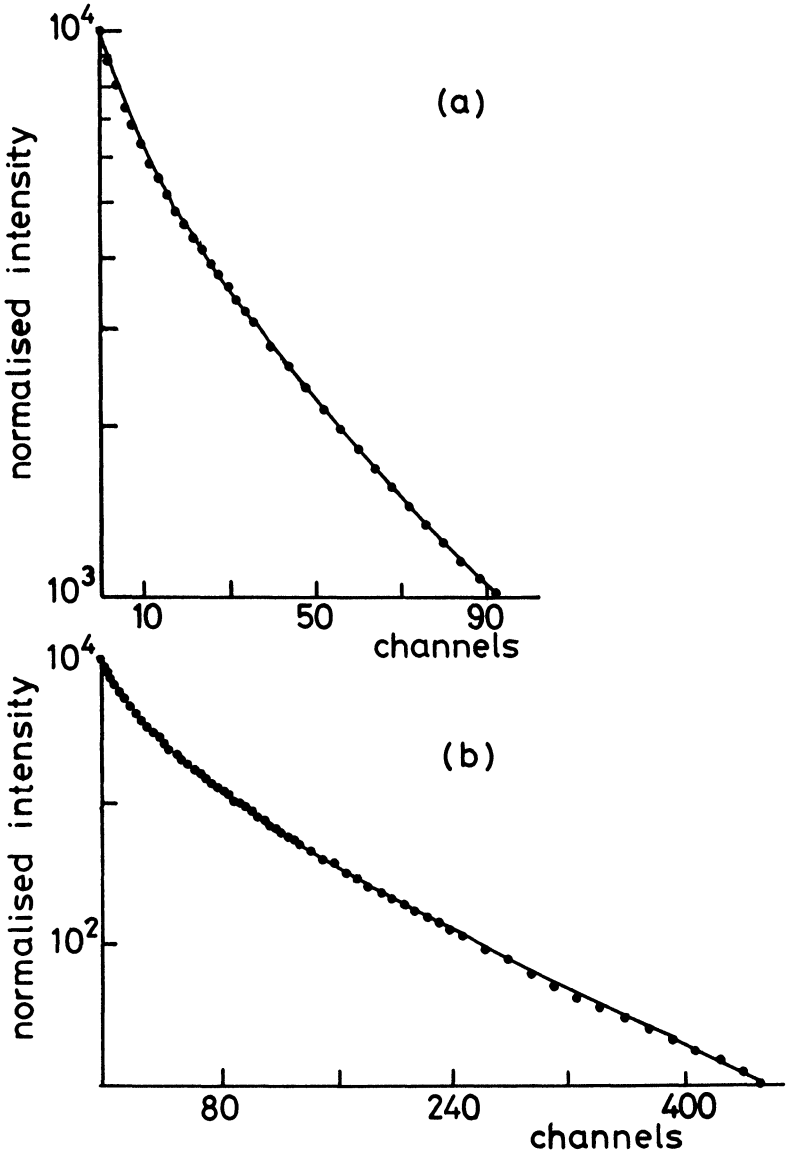

Figure 2 Comparison of the deconvoluted b^* decay profile (•) obtained from a three-exponential analysis with the curve from Eq. (1) using the data given in Table II for the system DMABN-0.5 mol dm^{-3} BuOH. The fit over the first decade (a) and over three decades (b) of intensity are shown.

To account for these observations, Scheme 3 has been devised. It is proposed that a DMABN-polar solvent complex is initially formed in either the ground or excited state. This complex reorganizes with a rate dependent on the initial complex geometry, to the geometry from which the excited state reaction, $b^* \rightarrow a^*$ can occur. This process probably involves a co-operative reorganization of the DMABN-solvent complex and an internal rearrangement of the DMABN molecule itself. Reverse relaxation steps are omitted for clarity. It is the former process, the distribution of quenching rates (represented by $\{k\}_i$), which results in the observed complex decay kinetics of the b^* state discussed above. It should be stressed that the occurrence of this step in the presence of a low concentration of polar solvent *implies an important role for specific solvent-solute interactions in the fluorescence spectroscopy of DMABN* in three component systems. The subsequent step (k_{fast}) results in the picosecond decay process, not resolved in these experiments, but discussed extensively in the literature.[6–10]

The final step in Scheme 3, (k_{SR}) implies the subsequent stabilization of the newly formed a^* state, which will also involve reorientation of the environment and, possibly, further internal reorganization of the DMABN moiety. This step can be correlated in neat polar solvents at low temperature with the wavelength dependence of the a^* fluorescence decay profile. This supports the idea that solvent-solute reorientation is important in these circumstances, which in turn suggests that the a^* state has a more polar character than the b^* state. It is also possible that the radiative rate constant for the a^* state will be sensitive to the extent of the reorientation, and could thus be time dependent.

These experiments established that *specific* solvent-solute interactions are required to explain the photophysics of DMABN in solution.

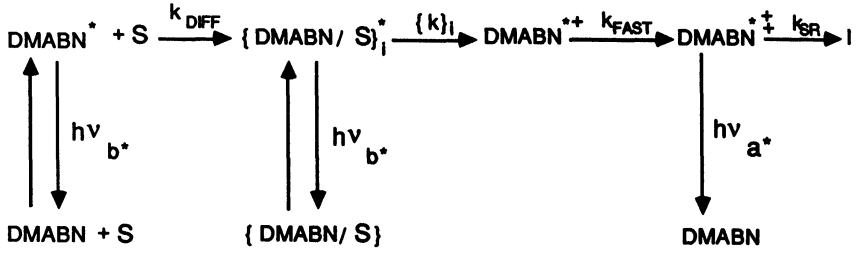

Scheme 3

We next turn to supersonic jet experiments where such specific interactions are probed in detail.

(b) Supersonic jet studies

In this section the results of laser induced fluorescence (LIF) studies of DMABN, 4-ABN and their solvated complexes are presented and discussed. A number of studies of jet-cooled DMABN have now been published.[17,19–21] Although no a^* emission has been observed, another type of anomalous behaviour has been revealed: the formation of both fluorescent and non-fluorescent solvated complexes depending on the nature of the intermolecular interaction. To assist in understanding the behaviour of jet-cooled DMABN we have also studied the related but simpler molecule, 4-ABN. TICT state formation does not occur in 4-ABN because of the higher ionization potential of the amino group.

THE DMABN AND 4-ABN BARE MOLECULES

The origin region of the fluorescence excitation of DMABN is shown in Figure 3(a); the lowest energy transition observed was at 32,333 ± 5 cm^{-1}. Similar spectra have been reported by Kobayashi *et al.*,[19] Peng *et al.*[20] and Warren *et al.*[21] The characteristic pattern of low frequency bands was repeated throughout the spectrum built on vibrations of 373, 494 and 780 cm^{-1}.[17] By analogy with 4-ABN (see below) these can be assigned as $6a_0^1$, $10b_0^2$, and 1_0^1 (using Varsanyi's notation[33]). The observation of virtually identical low frequency structure in the LIF spectrum of dimethylaniline[32] and the absence of this structure from the 4-ABN spectrum (Figure 3(b)) indicates that the low frequency transitions are associated with the dimethylamino group. An unequivocal assignment is impossible at present, but, as discussed elsewhere,[32] the prominent 60 cm^{-1} progression (Figure 3(a)) can be attributed to torsion of the dimethylamino group about the *N*-aryl bond. The activity of this mode in the excitation spectrum indicates that the S_1 state of DMABN is already twisted to some extent prior to formation of the a^* state. Dispersed fluorescence spectra following excitation of a number of vibronic transitions up to an excess vibrational energy of 840 cm^{-1} were recorded. In all cases a search was made as far as 12,000 cm^{-1} to the red of the resonance transition but no

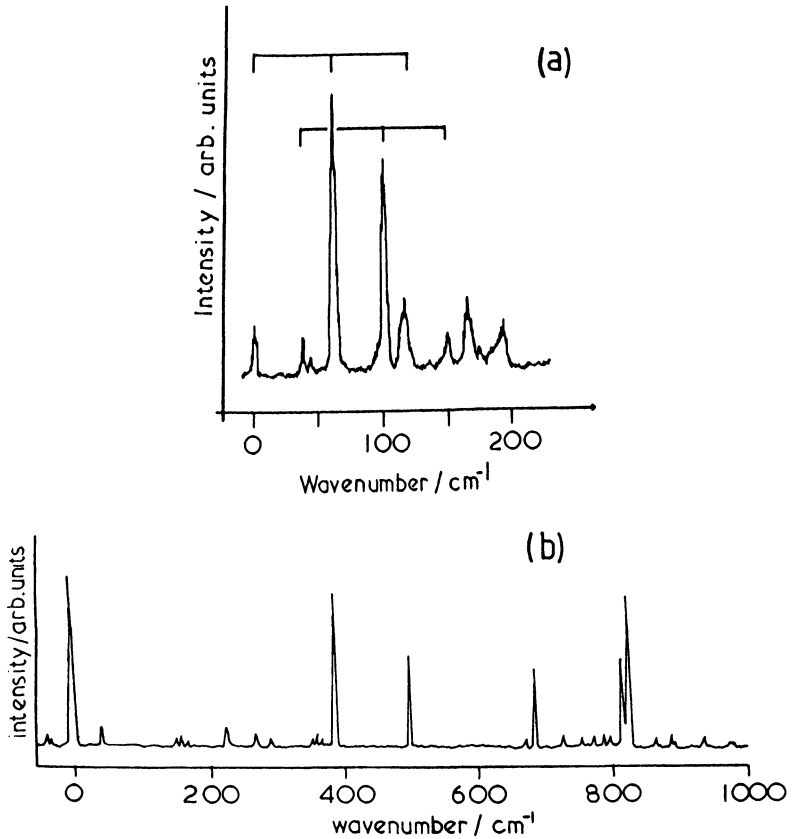

Figure 3 (a) The origin region of the fluorescence excitation spectrum of jet-cooled DMABN. Two progressions in 60 cm^{-1} are indicated. (b) The fluorescence excitation spectrum of jet-cooled 4-ABN.

emission which could be attributed to the a^* state was found, even when directly exciting torsional modes of the dimethylamino group. The absence of a^* state formation was confirmed by the essential invariance of the fluorescence lifetime across the excitation spectrum. As reported previously[17] the fluorescence of decay of jet-cooled DMABN was single exponential with lifetime in the range 5–6 ns over the excitation range $\Delta v = 0$ to 900 cm^{-1}. These lifetime values are in good agreement with those recently reported by Peng *et al.*[20] The

supersonic jet measurements conducted in this laboratory and elsewhere[19,20] thus confirm that solvation plays an essential role in the formation of the a^* state.

The fluorescence excitation spectrum of 4-ABN is shown in Figure 3(b). As remarked above, the absence of the *N*-methyl groups greatly simplifies the spectrum which closely resembles that of aniline.[34] The intense O_0^0 transition occurs at 33,493 ± 5 cm^{-1} and the spectrum is dominated by four totally symmetric fundamentals: $6a$(382 cm^{-1}), 12(678 cm^{-1}), 1(815 cm^{-1}) and 13(1164 cm^{-1}). The transition at 807 cm^{-1} can be assigned as I_0^2, the $\Delta v = 2$ transition in the amino inversion mode, as discussed elsewhere.[18] The inversion mode is also active in the dispersed fluorescence spectra following excitation of the O_0^0, $6a_0^1$, 12_0^1, 1_0^1, and 13_0^1 transitions; full assignments of these spectra are given in Ref. 18. The I_2^0 transition occurs at 430 cm^{-1}. The inversion frequencies observed for 4-ABN are comparable in magnitude to those of aniline[35] (via I_0^2 = 761 cm^{-1}, I_2^0 = 427 cm^{-1}) suggesting that the amino group of 4-ABN, like that of aniline, is pyramidal in the ground state, becoming quasi-planar in the S_1 state.[35]

SOLVATED COMPLEXES OF DMABN AND 4-ABN

The fluorescence excitation spectrum of the 1:1 DMABN-CH_3OH complex is shown in Figure 4. The spectrum is blue-shifted by 19 cm^{-1} relative to the bare molecule spectrum and exhibits identical low frequency structure. LIF spectra of DMABN-H_2O and DMABN-CF_3H complexes have been observed by Kobayashi *et al.*[19] and Peng *et al.*[20] have recently reported LIF of DMABN-NH_3 and DMABN-CH_3CN. Like DMABN-CH_3OH, these 1:1 complexes exhibited hypsochromic spectral shifts (summarized in Table III) and their spectra showed the same low frequency structure as the bare molecule. This latter observation suggests that the solvent molecule is interacting with the benzonitrile moiety rather than the dimethylamino group, and is thus not perturbing the low frequency oscillations. This argument is supported by the calculations of Lipinski *et al.*[36] which show that the dipolar charge distribution of the ground state is largely associated with the benzonitrile group and that excitation to the S_1 state results in a reversal of the local benzonitrile dipole, as a result of charge transfer from the dimethylamino group to the ring. This is consistent with the

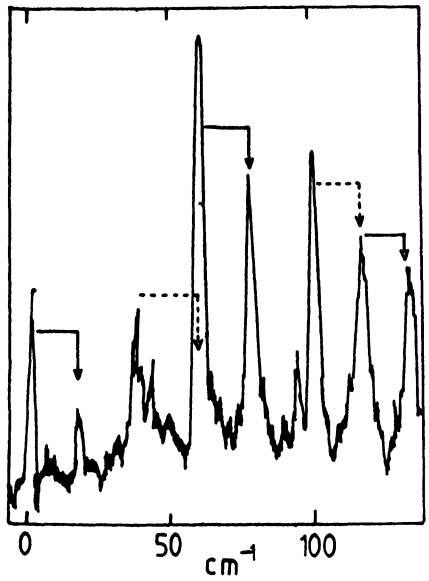

Figure 4 The origin region of the fluorescence excitation spectrum of the DMABN-CH_3OH complex. Complex features are indicated by arrows relative to the corresponding bare molecule features; dotted arrows indicate complex peaks which are concealed by bare molecule peaks.

Table III Microscopic solvent shifts exhibited by 1:1 DMABN-solvent complexes observed by LIF.

Ligand	$\Delta\nu/cm^{-1}$
CH_3OH	19
H_2O[ab]	18
CF_3H[a]	69
NH_3[b]	21
CH_3CN[b]	254

[a] Ref. 19.
[b] Ref. 20.

observed decrease in binding energy on excitation of the complexed DMABN. Since complexation of this type does not stabilize the S_1 (b^* state) then neither will it stabilize the a^* state; it is not surprising therefore that these complexes show only normal (b^*) fluorescence and the fluorescence lifetime of the DMABN-CH_3OH complex does

not differ significantly from that of the bare molecule. By increasing the partial pressure of methanol in the expansion we were able to form complexes of higher stoichiometry. The formation of such complexes was manifested by a decrease in the intensity of excitation features due to the bare molecule and 1:1 complexes. However, no new excitation features due to DMABN-CH_3OH complexes of 1:2 (or higher) stoichiometry could be found even when the excitation spectra of the bare molecule and the 1:1 complex had completely disappeared. Kobayashi *et al.*[19] reported similar behaviour with H_2O and CF_3H. Peng *et al.*[20] simply report that they were unable to observe complexes of greater than 1:1 stoichiometry.

We attributed the above behaviour to the formation of non-fluorescent 1:2 complexes between DMABN and CH_3OH, H_2O and CF_3H[18]. A recently published two colour time of flight mass spectrometric (TOFMS) study of DMABN complexes, by Warren *et al.*,[21] has confirmed this interpretation. The TOFMS of DMABN-H_2O complexes reveals the existence of both a 1:1 and a 1:2 complex which are not observed in LIF, in addition to the fluorescent 1:1 complex. The spectrum of the non-fluorescent 1:1 DMABN-H_2O complex is blue shifted 199 cm^{-1} relative to the bare molecule and displays low frequency structure which differs slightly from that of the bare molecule with some additional low frequency features occurring. The 1:2 DMABN-H_2O complex exhibits a blue spectral shift of 401 cm^{-1}.

Warren *et al.*[21] also investigated complexes between DMABN and the aprotic polar solvents acetonitrile and acetone. The TOFMS at 1:1 DMABN-CH_3CN revealed a blue-shifted complex feature at $\Delta\nu$ = 252 cm^{-1}, which was also observed in LIF[20], and a second *red-shifted* feature at $\Delta\nu = -900$ cm^{-1} whose spectrum does not resemble that of the bare molecule. Similar behaviour was observed for DMABN-$CH_3{\cdot}CO{\cdot}CH_3$, with a blue shift of 260 cm^{-1} and a red shift of -680 cm^{-1} in this case. The nature of the 1:1 complexes exhibiting these large bathochromic shifts is not clear and their fluorescence behaviour has yet to be reported, but it seems likely that they involve a solute-solvent interaction conducive to TICT state formation.

Some interesting comparisons can be made between the behaviour described above and that of 4-ABN-solvent complexes which will now be discussed. As shown in Table IV, 1:1 complexes between 4-ABN and CH_3CN, C_2H_5CN and C_3H_7CN exhibited blue solvent shifts of around 240 cm^{-1}, similar to that observed for DMABN-CH_3CN. The

Table IV Microscopic solvent shifts exhibited by 4-ABN-solvent complexes.

Ligand	$\Delta\nu/cm^{-1}$
CH_3CN	236
C_2H_5CN	239
i-C_3H_7CN	238
H_2O	84
	196
	314
CH_3OH	92
	210
	215
	239
	249
	305

intermolecular interaction in these complexes is expected to be dipole–dipole in nature and the decrease in binding energy on excitation can be rationalized in terms of the change in charge distribution as discussed above for DMABN. No red-shifted feature, like that seen by TOFMS for DMABN-CH_3CN[21], was found.

For 4-ABN-H_2O, three blue-shifted 1:1 complex excitation bands were observed (see Table IV and Figure 5(a)). The rotational contours of these three excitation features are shown in Figure 6, in comparison with that of the bare molecule O_0^0 band. All three show B-type rotational contours which are narrower than that of the bare molecule and the width of the contours decreases with increasing spectral shift. The fact that the three excitation features have different rotational profiles shows that they are due to three different geometrical isomers, rather than being vibronic transitions of the same complex. Two obvious types of intermolecular interaction could give rise to the blue shifts observed here: hydrogen bonding to the cyano group or to the amino nitrogen. AM1 calculations have been performed to predict some possible stable complex geometries involving such interactions. Four examples of stable configurations are shown schematically in Figure 7. Of the two obvious alternative structures for interaction at the cyano group, Figure 7(a) and (b), the linear structure, (a), is predicted to be more stable. A number of possible configurations can be envisaged for hydrogen bonding to the amino nitrogen, two

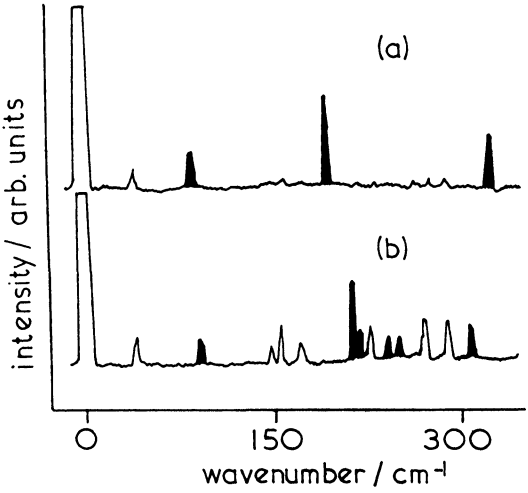

Figure 5 Fluorescence excitation spectra of (a) DMABN-H_2O, (b) DMABN-CH_3OH. The complex features are shaded to distinguish them from those of the bare molecule.

examples of stable geometries are shown in Figure 7(c) and (d). Further AMl calculations and rotational contour simulation are being undertaken to yield more detailed structural information; at this stage it seems likely that in one of the observed complexes water is hydrogen bonded to the cyano group and the other two involve interaction with the amino nitrogen.

The LIF spectrum of 4-ABN-CH_3OH (Figure 5(b)) resembles that of 4-ABN-H_2O (Figure 5(a)), although some additional features are present (see Table IV). The prominent bands at 92, 210 and 305 cm^{-1} are thought to correspond to complexes similar in structure to those observed for 4-ABN-H_2O discussed above. The rotational contours of these peaks are similar in shape to those of the 4-ABN-H_2O complexes and show a similar decreasing width with increasing spectral shift. The weaker features to the blue of the 210 cm^{-1} band could be due to intermolecular vibrational transitions.

Returning now to DMABN, we are led to the following conclusions regarding its complexation behaviour. Like 4-ABN, DMABN can form stable hydrogen-bonded complexes involving interaction at either the cyano group of the amino nitrogen. Interaction of a protic

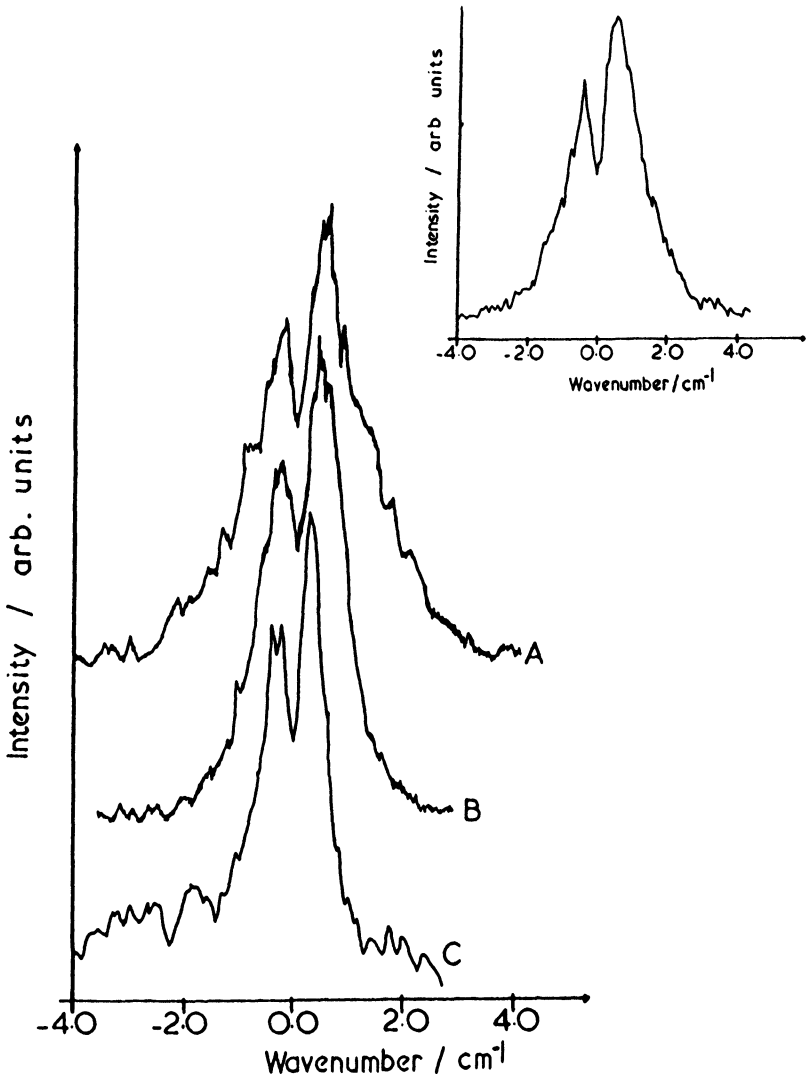

Figure 6 Rotational contours of the 4-ABN-H_2O excitation features occurring with spectral shifts of (a) 84 cm^{-1}, (b) 196 cm^{-1}, and (c) 314 cm^{-1}. The inset shows the rotational contour of the bare molecule O_0^0 transition, for comparison. 4-ABN is a near symmetric top and the $S_1 \leftarrow S_0$ transition is short axis polarized (perpendicular to the top axis) giving rise to a *B*-type rotational contour.

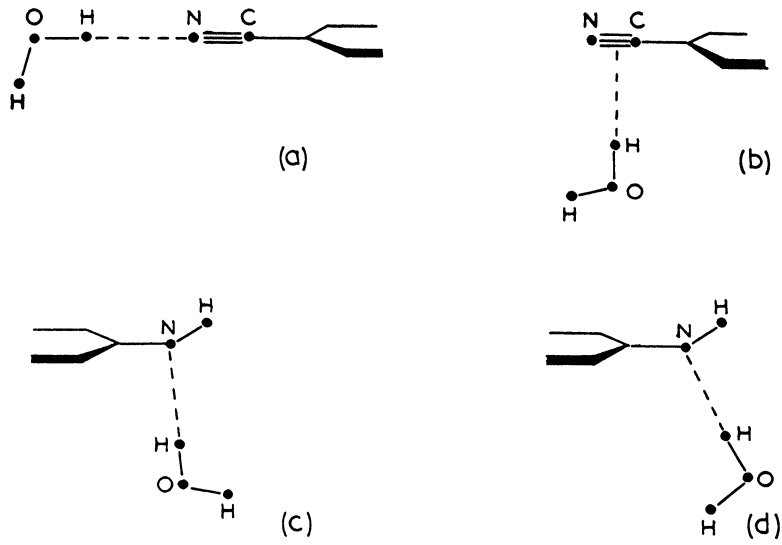

Figure 7 Schematic representation of AMl optimized geometries of 4-ABN-H_2O complexes. In (b), (c) and (d) the water molecule lies below the plane of the aromatic ring.

solvent molecule, such as H_2O, CH_3OH etc., with the cyano group produces a fluorescent complex; interaction at the dimethylamino nitrogen, however, results in formation of non-fluorescent complexes (hence the 1:1 and 1:2 DMABN-H_2O complexes observed in TOFMS but not LIF). This fluorescence quenching, which does not occur in 4-ABN, appears to specifically involve the dimethylamino group. A possible mechanism for the solvent induced non-radiative decay could be rapid relaxation of the initially excited state to an exciplex state which is non-fluorescent (or too weakly fluorescent to be observed) under jet-cooled conditions. As discussed earlier, an alternative to the TICT model has been proposed which attributes the a^* emission to a DMABN-solvent exciplex which involves interaction of lone pair orbitals on the amino group and solvent molecule.[13]

Interaction of DMABN with an aprotic polar solvent molecule such as CH_3CN results in different behaviour. Only one blue-shifted 1:1 complex is formed; this is fluorescent and is thought to involve dipole–dipole interaction with the benzonitrile moiety. In addition a

strongly red-shifted absorption feature due to a 1:1 complex has been observed; the nature of this complex is not yet clear but it may prove to be a precursor of the TICT state. Thus, although a^* emission has not yet been observed from a jet-cooled complex of DMABN, these experiments have revealed that specific solute-solvent interactions strongly influence the photophysical behaviour of this molecule.

Acknowledgements

We are grateful to the Science and Engineering Research Council for generous financial support, and to erstwhile and present colleagues Stephen Meech, Elizabeth Gibson, Alan Taylor and Wim Bouwman for their contributions to this work.

References

1. E. Lippert, M. Luder and H. Boos in "Advances in molecular spectroscopy" Ed. Mangini, Pergamon, p. 443 (1962).
2. K. Rotkiewitz, K. H. Grellman and Z. R. Grabowski, *Chem. Phys. Lett.* **19**, 315 (1973); K. Rotkiewitz, A. Krowczynski and W. Kuhnle, *J. Lumin.* **12–13**, 877 (1976).
3. W. Rettig, G. Wermuth and E. Lippert, *Ber. Bunsenges. Phys. Chem.* **83**, 692 (1979).
4. W. Rettig, *Agnew. Chem. Int. Ed. Engl.* **25**, 971 (1986).
5. Z. R. Grabowski, K. Rotkiewicz, W. Rubaszewska and E. Kirkurkaminoska, *Acta Phys. Polonica.* **A45**, 767 (1978).
6. Y. C. Wang and K. B. Eisenthal, *J. Chem. Phys.* **77**, 6076 (1982).
7. Y. C. Wang, M. J. McAuliffe, F. Novak and K. B. Eisenthal, *J. Phys. Chem.* **85**, 3736 (1981).
8. J. Hicks, M. Vanderscill, Z. Babarogic and K. B. Eisenthal, *Chem. Phys. Lett.* **116**, 18 (1985).
9. D. Huppert, S. Rand, P. M. Rentzepis, P. Barbara, W. Struve and Z. R. Grabowski, *J. Photochem.* **75**, 5714 (1981).
10. E. M. Kosower and D. Huppert, *Chem. Phys. Lett.* **96**, 433 (1983).
11. F. Heisel and J. A. Miehe, *Chem. Phys.* **98**, 233 (1985).
12. E. A. Chandross, in "The exciplex" Eds. M. Gordon and W. R. Ware, Academic Press, New York, 187 (1975).
13. R. J. Visser, C. A. G. O. Varma, J. Konijnenberg and P. Bergwerf, *J. Chem. Soc. Faraday II* **79**, 347 (1983).
14. R. J. Visser, P. C. M. Weisenborn and C. A. G. O. Varma, *Chem. Phys. Lett.* **132**, 330 (1985).
15. S. R. Meech and D. Phillips, *Chem. Phys. Lett.* **116**, 263 (1985).
16. S. R. Meech and D. Phillips, *J.C.S. Faraday* **2**, 83 (1987).
17. E. M. Gibson, A. C. Jones and D. Phillips, *Chem. Phys. Lett.* **136**, 454 (1987).
18. E. M. Gibson, A. C. Jones and D. Phillips, *Chem. Phys. Lett.* **146**, 270 (1988).
19. T. Kobayashi, M. Futakamic and O. Kajimoto, *Chem. Phys. Lett.* **130**, 63 (1986).
20. L. W. Peng, M. Dontus, A. H. Zewail, K. Kemnitz, J. M. Hicks and K. B. Eisenthal, *J. Phys. Chem.* **91**, 6162 (1987).
21. J. A. Warren, E. R. Bernstein and J. I. Seeman, *J. Chem. Phys.* **88**, 871 (1988).

22. W. Rettig, M. Noyel, E. Lippert and H. Otto, *Chem. Phys.* **103**, 381 (1986).
23. R. A. Lampert, L. A. Chewter, D. Phillips, D. V. O'Connor, A. J. Roberts and S. R. Meech, *Anal. Chem.* **55**, 68 (1983).
24. D. V. O'Connor and D. Phillips, "Time-correlated single photon counting" Academic Press, NY 1984.
25. A. R. Auty, A. C. Jones and D. Phillips, *Chem. Phys. Lett.* **112**, 529 (1984).
26. M. J. S. Dewar, E. G. Zoebisch, E. F. Healy and J. J. P. Stewart, *J. Am. Chem. Soc.* **107**, 3902 (1985).
27. D. R. James and W. R. Ware, *J. Phys. Lett.* **120**, 455 (1985); **126**, 7 (1986).
28. A. Siemiarczak and W. R. Ware, *J. Phys. Chem.* **91**, 3677 (1987).
29. R. Kohlrausch, *Ann. Phys.* **12**, 393 (1847).
30. G. Williams, D. C. Watts, S. B. Dev and A. M. North, *Trans. Faraday Soc.* **67**, 1323 (1971).
31. G. Williams and D. C. Watts, *Trans. Faraday Soc.* **65**, 80 (1969).
32. E. M. Gibson, A. C. Jones, A. G. Taylor, W. G. Bouwman, D. Phillips and J. Sandell, *J. Phys. Chem.* **92**, 5449 (1988).
33. G. Varsanyi, "Assignments for vibrational spectra of seven hundred benzene derivatives" (Wiley, New York, 1974).
34. N. Mikami, A. Hiraya, I. Fujiwara and M. Ito, *Chem. Phys. Lett.* **74**, 531 (1980).
35. J. M. Hollas, M. R. Howson, T. Ridley and L. Halonen, *Chem. Phys. Lett.* **98**, 611 (1983).
36. J. Lipinski, H. Chojnacki, Z. R. Grabowski and K. Rolkiewicz, *Chem. Phys. Lett.* **70**, 449 (1980).